Impact of Communication Path Loss to Unmanned Aircraft Swarm Coherency

Allison Hudak
Noblis
Washington, D.C.
allison.hudak@noblis.org

Scott James
Noblis
Washington, D.C.
scott.james@noblis.org

Robert Raheb
Noblis
Washington, D.C.
robert.raheb@noblis.org

***Abstract*—This work examines the impact of communicative path loss to the coherency of Unmanned Aircraft (UA) swarms within constrained, urban environments. Within swarm formations, UAs must remain close enough to communicate their position to other swarm constituents while maintaining sufficient separation to avoid collision. We analyze the tension between these two separation considerations, comparing different communication protocols and trajectory planning algorithms. With these considerations, we demonstrate the impact of increased swarm sizes on swarm coherence.**

***Index Terms*—UTM, UA, Swarm, CV2-X, 802.11p**

I. Overview

Swarm coherency, or the ability for constituent UAs to coordinate with the swarm, is dependent on the ability of UAs to communicate their position to one another. We assume that UAs communicate their position through discrete information packets and must communicate with each UA. Communication between UAs is inhibited by path loss. The major factor in our path loss model is distance. As path loss increases with distance, so will the probability of packet loss. Therefore, as path loss increases, we expect swarm coherency to decrease as the ability to communicate is diminished.

Our path loss model will consider operational measurements from two communication technologies currently under consideration for supporting UA operations beyond line of sight (LOS) initiatives: Cellular-Vehicle-to-Everything (C-V2X) and IEEE 802.11p. Note that we are not modeling the determination of communication factors, but instead examining the sensitivity of swarm coherency to these factors.

We will apply this model to two different trajectory planning algorithms:

1) Optimal Reciprocal Collision Avoidance (ORCA) [1]: a velocity-based algorithm
2) D* [3]: 3D grid-based, incremental approach commonly used in autonomous vehicle navigation

Our approach will be to:

1) Calibrate a well clear buffer for each algorithm that maintains safe separation between UAs
2) Determine how the swarm formations managed by algorithms and their associated buffers are impacted by the path loss curves for each communication technology

TABLE I
Path Loss Parameters derived from [4, Fig. 2(a)]

Technology	Power	c1	c2
802.11p	8 dB	0.1	110
802.11p	23 dB	0.02	200
C-V2X	8 dB	0.05	120
C-V2X	23 dB	0.015	150

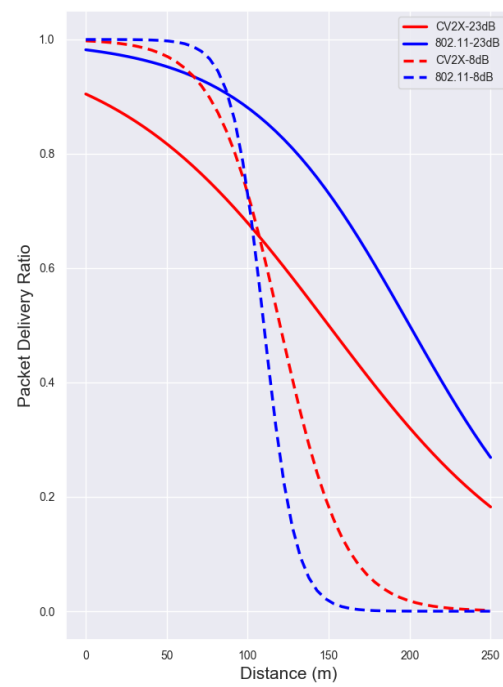

Fig. 1. Packet Delivery Ratio over Distance by Power Curve

II. Path Loss

We will model path loss, $PL(d)$ by the equation:

$$PL(d) = (1 + e^{c_1(c_2 - d)})^{-1}$$

where d is distance in meters and c_1 and c_2 are factors derived from the power curves for each communication technology [4, Fig. 2(a)]. The output is the probability of packet loss.

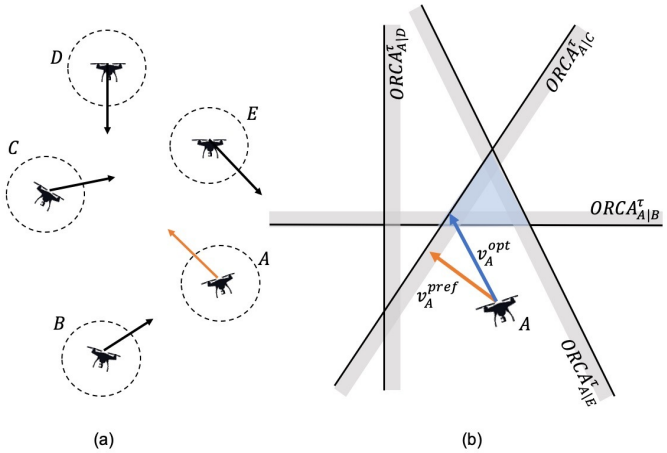

Fig. 2. ORCA UA Diagram

From the path loss equation, we derive the Packet Delivery Ratio (PDR): the number of packets received over the total packets sent, or the complement of packet loss:

$$PDR(d) := 1 - PL(d)$$

The PDR curves for the communication technologies in Table I are shown in Figure 1.

III. The Algorithms

A. ORCA

Optimal Reciprocal Collision Avoidance (ORCA) is a velocity-based approach to provide collision-free UA motion [1]. Each UA constructs a region that will not cause collisions with neighboring UAs (Figure 2). The region is constructed by considering the current velocity of each UA and determining what future positions are possible within a fixed time window. Within the allowed area of travel, each UA can select its preferred velocity.

B. D*

D* (D-Star) is a discretized grid-based approach for trajectory planning [3]. In our implementation of D*, this is performed by "snapping" each UA's location and destination to the closest 3D point in a defined grid. Note that this snapping is only performed for the purpose of trajectory planning. UAs do not "hop" from point to point, but instead move using a continuous physics model, guided toward intermediate destinations resultant from the trajectory planning.

An example of a grid along a single street is shown in Figure 3. Paths are calculated based on the shortest path to target in the grid. UAs avoid collision with other UAs by blocking grid points from their path that could cause collisions. The grid granularity impacts the ability to avoid collision. The UAs must be directed to move towards a grid point on its route of intended travel. If the grid points are spaced too far apart, the ability to change course and avoid other UAs is hampered. We use a five meter distance between grid points to conduct our experiments.

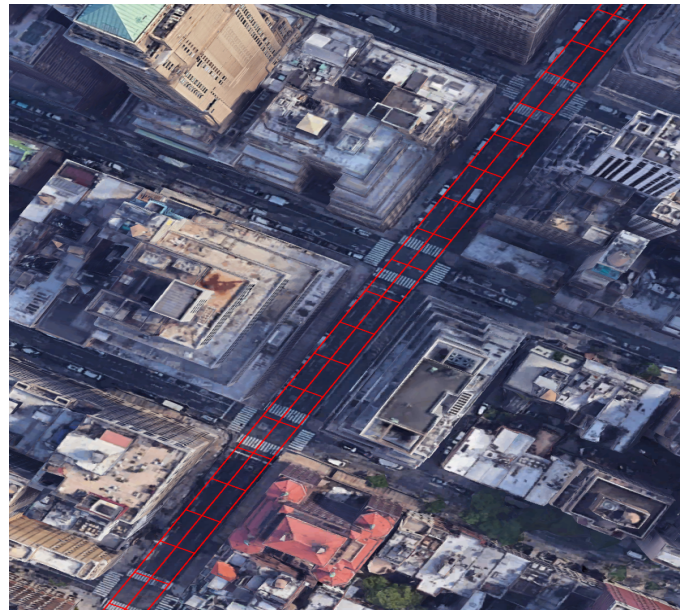

Fig. 3. Single Street D* Grid

There are differences in how ORCA and D* are implemented, including the time window in ORCA and the grid granularity in D*. Varying these parameters will produce different results for our experimental scenarios. Our motivation is not to produce an exhaustive comparison between the two algorithms but rather to demonstrate how communication path loss impacts different trajectory planning mechanisms.

IV. Trajectory Planning Engine

We incorporated the above communication parameters and algorithms into a trajectory planning engine. This engine is a discrete event simulator for the purpose of running multi-UA trajectory planning scenarios within geographically restricted regions using parameterizable communication constraints. The engine generalizes the key operational inputs that are shared between the different algorithms. The engine was executed using a High-Performance Computer (HPC) during complex and high traffic volume scenarios. While the engine does support LOS, this is not a factor in our scenarios as the UAs will be positioned within a single open street.

V. Calibration

We first calibrate the safe operational separation for the UA swarms. To do this, we consider a scenario where two UA swarms approach head-on (Figure 4) and then pass through each other (Figure 5). We define a Near Midair Collision (NMAC) as two UAs violating a five meter separation [7]. In other words, the smallest distance by which two UAs should ever be separated is five meters. For each algorithm, we introduce and vary a well clear buffer to ensure that NMACs do not occur [8].

The well clear buffer is a multiple of the NMAC separation value and acts as a trigger for UAs to begin deconflicting with other UAs. The pass-through scenario is an extreme case

Fig. 4. Swarms Meet

Fig. 5. Swarms Pass Through

by which to determine a suitable buffer. If the UAs are able to maintain safe separation greater than five meters in this scenario, it is likely they can maintain a safe separation in less extreme cases with a similar number of UAs and not result in a NMAC. The inter-swarm measurements consider distances between members of different swarms. In Figure 6, the inter-swarm minimum separation is graphed over time for D* with varying buffer multiples. The buffer of three times the NMAC separation value stays above five meters and is therefore adequate for our calibration purposes to maintain safe separation. Increasing the buffer to maintain a safe inter-swarm separation causes the intra-swarm separation to increase as shown in Figure 7 [7].

In the same manner, we calibrated the buffer for ORCA as two times the NMAC separation value as seen in Figure 8. The difference between the buffer requirements for D* and ORCA can be attributed to ORCA's variable velocity and the grid resolution chosen for D*. The variable velocity in ORCA allows the UAs to slow down when navigating around each other, whereas in our implementation, D* is restricted to either traveling a single speed or stopping completely.

The common simulation parameters are defined in Table II.

TABLE II
UA CONSTRAINTS

Qualifier	Measurement	Value
min	speed	0 knots (stationary)
max	speed	13 knots (24 km/hour)
min	NMAC	5 meters

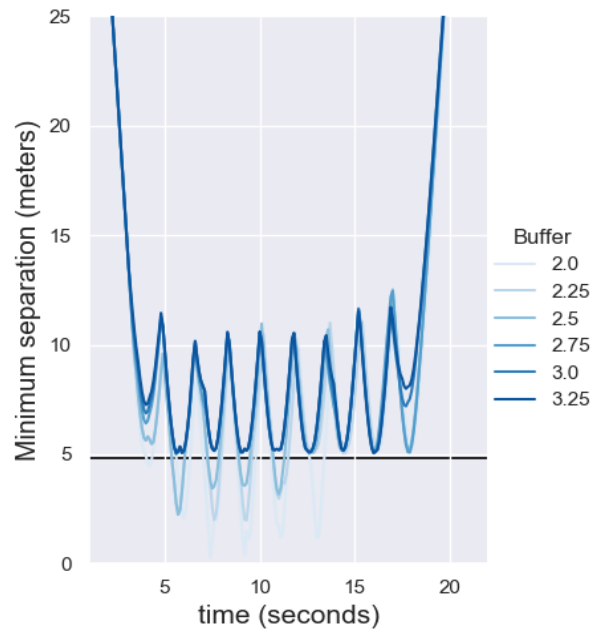

Fig. 6. Inter-Swarm Minimum Separation for D* Varying Buffer

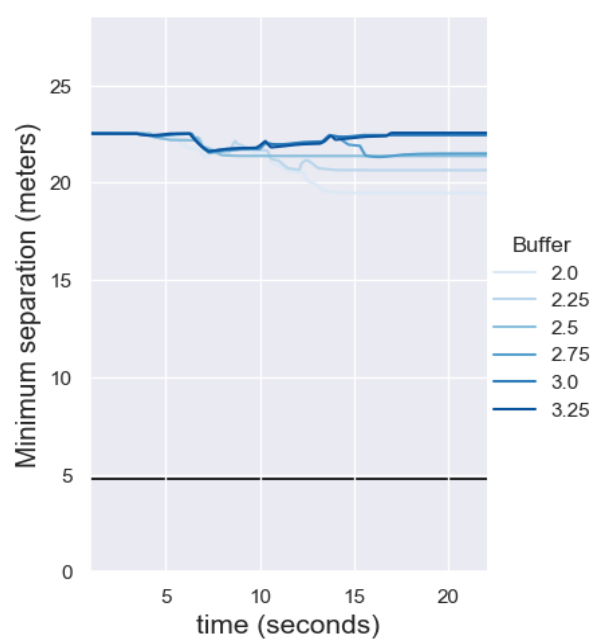

Fig. 7. Intra-Swarm Minimum Separation for D* Varying Buffer

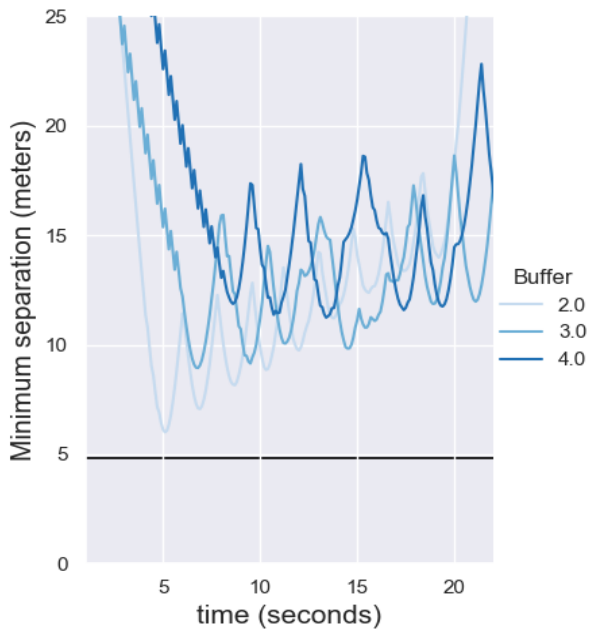

Fig. 8. Inter-Swarm Minimum Separation for ORCA Varying Buffer

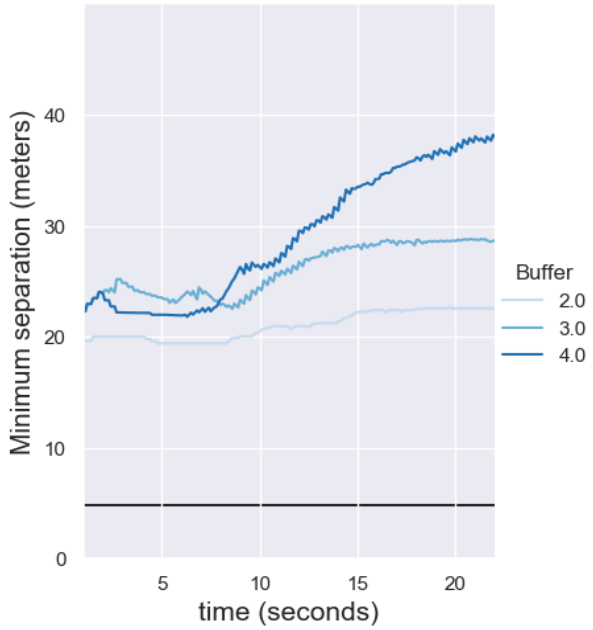

Fig. 9. Intra-Swarm Minimum Separation for ORCA Varying Buffer

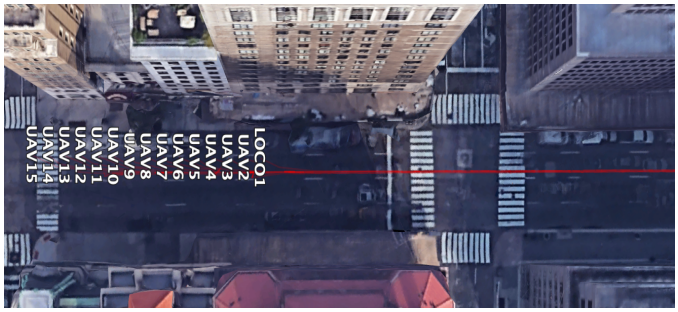

Fig. 10. Initial Positions of UAs in Single Swarm

VI. Determination of Functional Swarm Size

With the buffer calibrated, we examine how the functional size of the swarm is impacted by path loss. We do this by varying the number of UAs in a swarm and measuring its coherency via PDR.

We test a scenario using two communication technologies at two power levels [4, Fig. 2(a)]. The values are shown in Table I. The scenario starts with the swarm as a single line of UAs: effectively a swarm "train" (Figure 10). We intentionally place the UAs close together to force the algorithms to deconflict and to have the swarm start with as high of a PDR as possible.

We then allow the swarm train to advance forward. Initially, we expect little packet loss as the spatial size of the swarm will be small enough that path loss will be minimal. In other words, their close proximity allows for a high PDR. As the swarm continues forward, UAs will begin to separate (Figure 11) in order to reach their target well clear buffer. This will increase the spatial size of the swarm and introduce path loss. For small swarms, we will expect the PDR to remain relatively steady, whereas for large swarms we expect the PDR to drop as more UAs are farther apart from each other. Whereas we do consider building structures and LOS within our engine, these are not factors in our scenarios, as we are only considering simplified swarm geometries within the center of a single street.

The power curves we use in Figure 1 are validated in our model through our calibration scenario results which are plotted in Figure 12. With a power level of 8 dB, the PDR is near one within a close range (less than fifty meters) and it has a steep drop off outside of that range. The higher power level of 23 dB has a shallower slope which allows for a higher PDR at longer distances.

We vary the number of UAs in the single swarm scenario from 10 to 35. As the number of UAs increases, the maximum separation between UAs increases as shown in Figure 13. We next discuss the impact of increasing separation on PDR for each algorithm and communication technology.

A. ORCA Single Swarm Results

The PDR timeline for using ORCA at 8 dB is shown in Figure 14 for 802.11p and Figure 15 for C-V2X.

In both 8 dB scenarios, as the number of UA increases, the PDR shows substantial deterioration. For a 10 UA swarm, 802.11p at 8 dB maintains a PDR close to one, unlike C-V2X

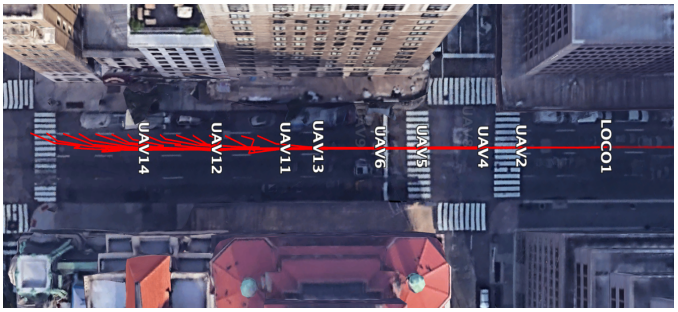

Fig. 11. UAs Spread Out in Single Swarm

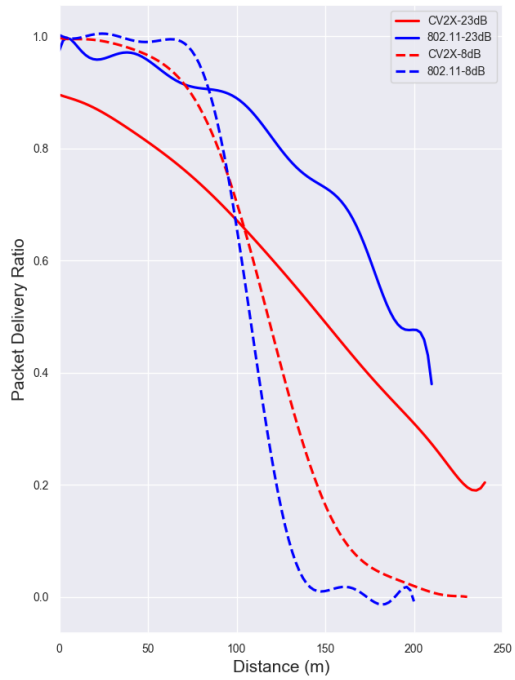

Fig. 12. Packet Delivery Ratio over Distance from Experiments

at 8 dB. This is due to the power curve for 802.11p at 8 dB being closer to one for a longer distance than C-V2X. Ten UAs remain within a range of high PDR for 802.11p.

In contrast to 8 dB, the shallow slopes for 23 dB depicted in Figure 1 are reflected in ORCA's results in Figure 16 and 17. The swarms do not start close to a PDR of one and have less change in PDR over time in comparison to 8 dB. At the highest number of UAs for CV2-X, the PDR dropped to under 75 percent. 802.11p at 23 dB has the least difference in PDR over time. At each swarm size, the PDR is over 90 percent.

Figure 18 diagrams the impact of larger swarm sizes. At 10 UAs, the swarm spreads out to maintain a safe separation within a distance that still allows for a high PDR. At 35 UAs, there are more pairs of UAs that are far apart to maintain safe separation in the swarm. The pairs of UAs toward the front and back of the swarm experience the most packet loss and lower the overall PDR.

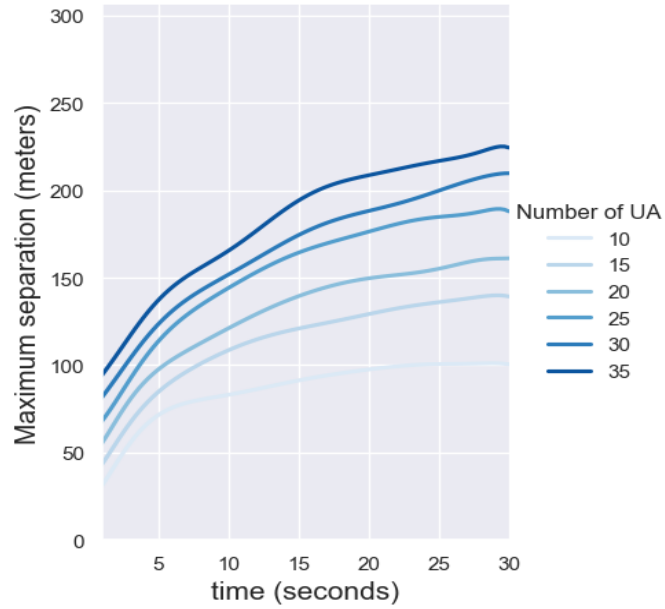

Fig. 13. Maximum Separation of UAs over Time

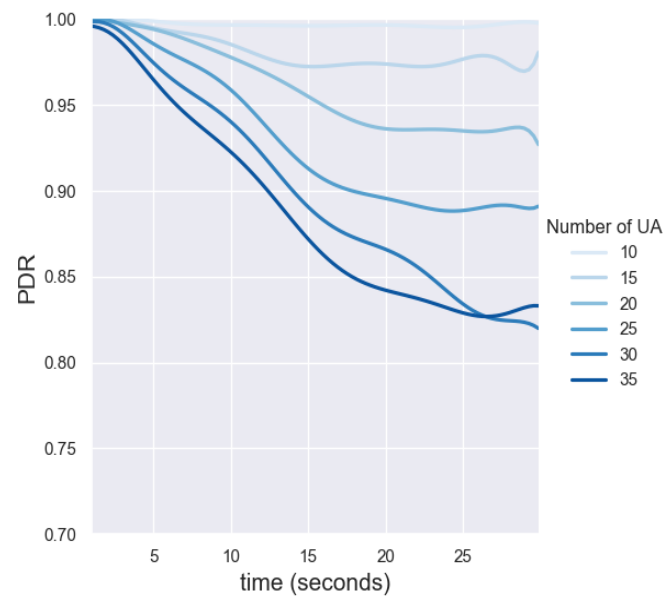

Fig. 14. ORCA 802.11p 8dB

B. D* Single Swarm Results

The results for D* are similar to ORCA in terms of the general shape of the PDR curves. A key difference is with 802.11p at 8 dB in Figure 19. Particularly with greater than 30 UA, the PDR drops as expected, but it does not begin to flatten out like ORCA in Figure 14. A flatter curve at the end implies that the UAs have reached a steady-state after spreading out above the buffer. Since D* does not show this behavior, the swarm is still deconflicting and spreading further apart. This is due to the comparatively larger buffer for D* versus ORCA. This causes the swarms in D* to reach a distance where there

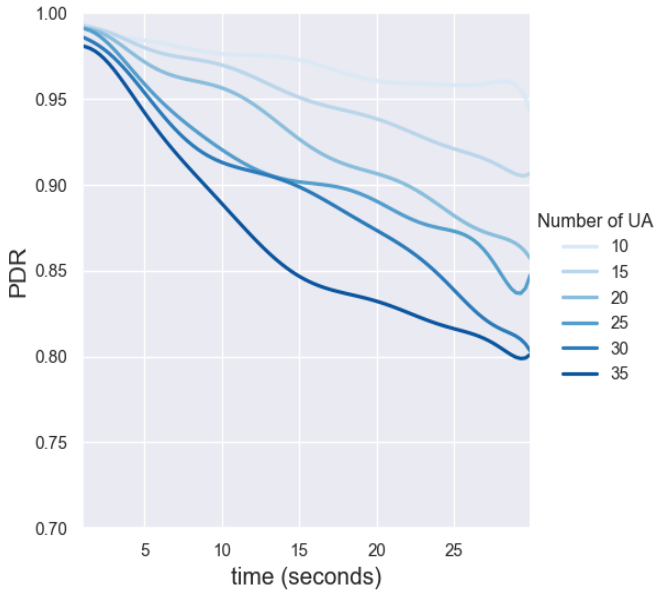

Fig. 15. ORCA C-V2X 8dB

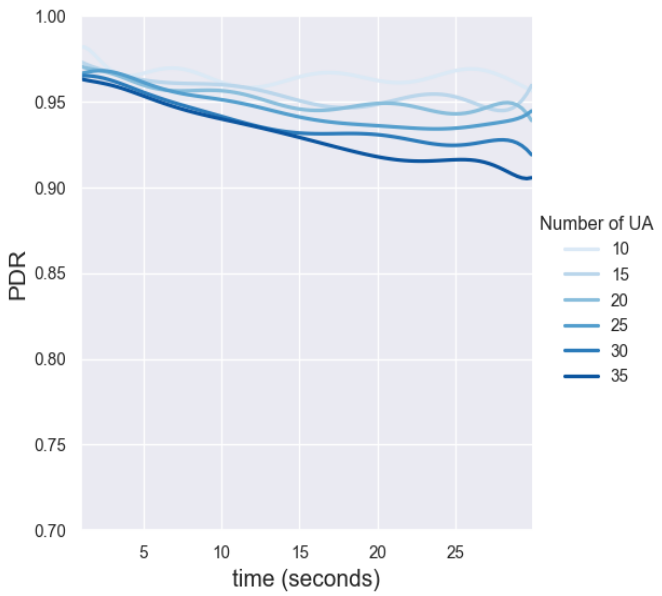

Fig. 16. ORCA 802.11p 23dB

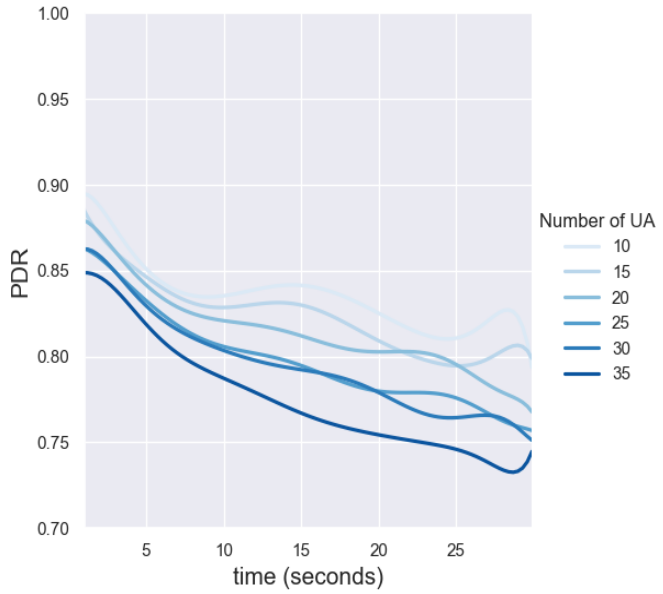

Fig. 17. ORCA C-V2X 23dB

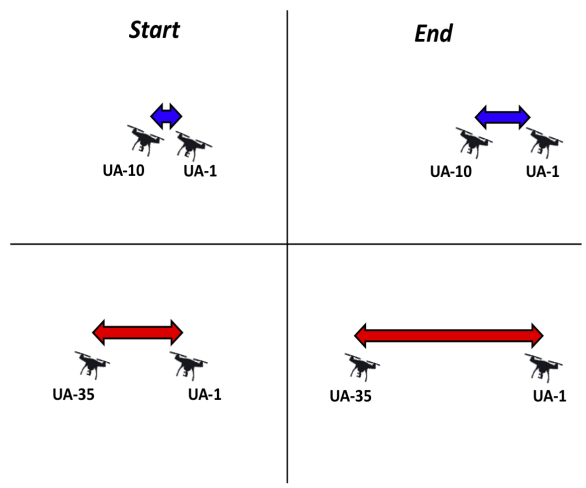

Fig. 18. Visual Diagram of Results

is a great drop off in PDR with 802.11p at 8 dB. The D* results for 802.11p and C-V2X at 23 dB in Figure 21 and 22 are similar to ORCA. This is expected as the PDR for these communication technologies are not as affected by distance.

VII. Conclusions and Future Work

Measuring the coherency of swarm behavior is a surrogate for the effectiveness of many vehicle-to-vehicle operational performance. As more UAs enter into the urban airspace, paradigms for their safe operation are being considered.

For swarms to function as a unit, their coherency must be maintained. UAs must not stray too far from their swarm else risk losing communication with other swarm members due to path loss and UAs must remain sufficiently separated from other swarms members else risk collision.

We explored the tension between safe separation and swarm compactness using the ORCA and D* path planning algorithms and operational parameters for CV2-X and 802.11p. Safe buffers limit swarm density, thus large swarm membership sizes will require larger spatial sizes and a subsequent deterioration of PDR. We saw that the power levels for communication technologies is also a consideration for swarm coherence. While higher power levels will produce higher

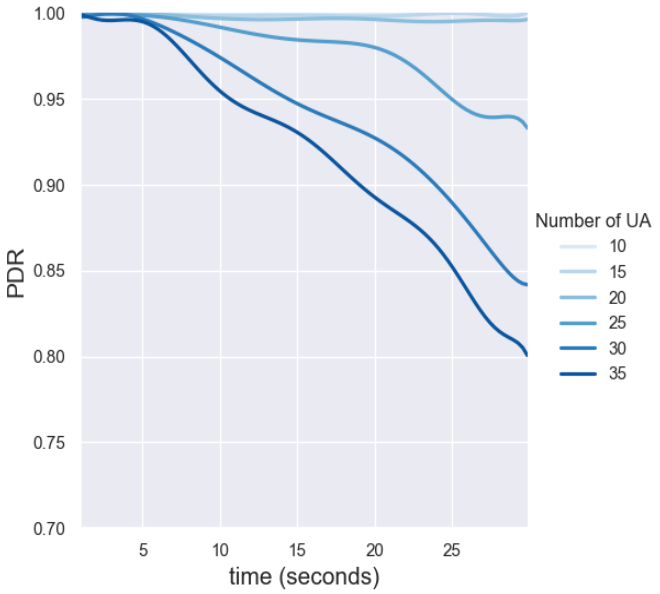

Fig. 19. D* 802.11p 8dB

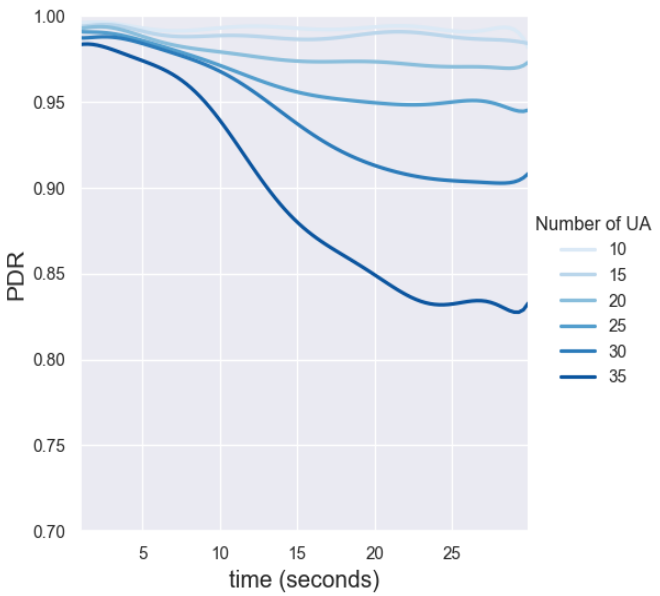

Fig. 20. D* C-V2X 8dB

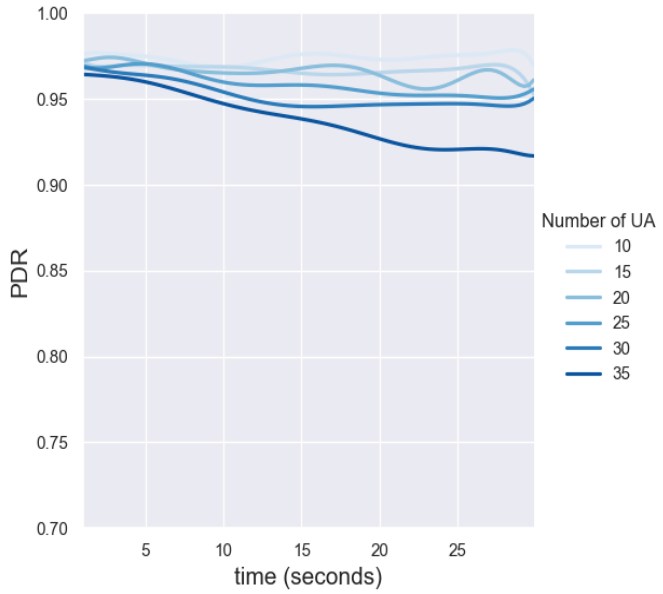

Fig. 21. D* 802.11p 23dB

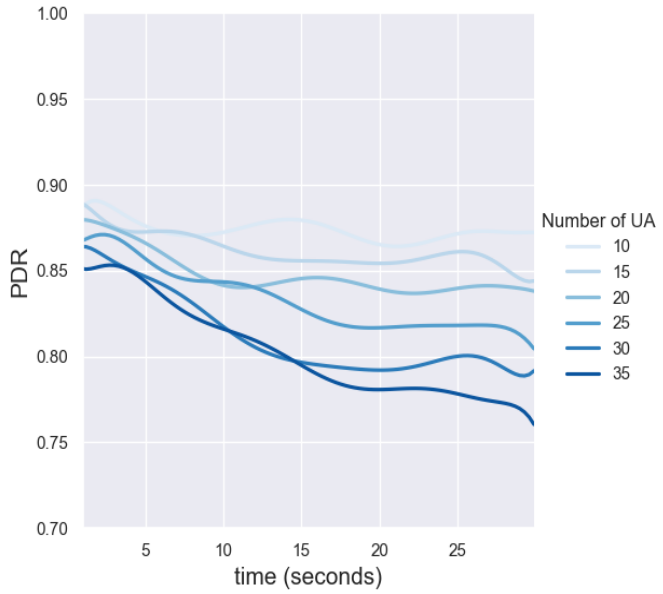

Fig. 22. D* C-V2X 23dB

PDR at larger distances, lower power levels provide more consistently high PDR within shorter ranges. Balancing high coherence against larger swarm sizes will be a consideration in tightly constrained urban corridors.

While we focused on distance as the main factor impacting communication between UAs, in future work we will expand our communication model to include other factors such as obstacles interfering with LOS. Additionally, this paper considered only direct connections between UAs. In future papers we will consider more complex communication between swarm members examining how different Mobile Ad Hoc Networks (MANETs) topologies impact UA swarm coherence.

References

[1] J. van den Berg, S. Guy, M. Lin, and D. Manocha. "Reciprocal n-body Collision Avoidance" May 7, 2011. http://gamma.cs.unc.edu/ORCA/publications/ORCA.pdf

[2] J. van der Berg, S. Guy, J. Snape, M. Lin, and D. Manocha. "RVO2 Library:Reciprocal Collision Avoidance for Real-Time Multi-Agent Simulation" May 2008. http://gamma.cs.unc.edu/RVO2/

[3] K. Al-Mutib and E. Mattar. "D* Lite Based Real-Time Multi-Agent Path Planning in Dynamic Environments" March 2012. https://www.researchgate.net/publication/236897587_D_Lite_Based_Real-Time_Multi-Agent_Path_Planning_in_Dynamic_Environments

TABLE III
LIST OF ABBREVIATIONS

Acronym	Expansion
C-V2X	Cellular-Vehicle-to-Everything
ORCA	Optimal Reciprocal Collision Avoidance
Multi-Agent D*	Multi-Agent D Star
PDR	Packet Delivery Ratio
UA	Unmanned Aircraft
UTM	UAV Traffic Management

TABLE IV
SPECIFIC USAGE OF TERMS IN THIS PAPER

Acronym	Usage
ORCA	velocity-based deconfliction algorithm
D*	discretized grid-based deconfliction algorithm
UA	a drone, a member of a swarm

[4] A. Bazzi. "Congestion Control Mechanisms in IEEE 802.11p and Sidelink C-V2X" Jan 2020. https://arxiv.org/pdf/2001.08495.pdf

[5] S. James, R. Raheb, "Path Planning for Critical ATM/UTM Areas" 38th Digital Avionics Systems Conference (DASC) September 8-12, 2019

[6] S. James, R. Raheb, A. Hudak "UAV Swarm Path Planning" Integrated Communications Navigation and Surveillance (ICNS) September 9-11, 2020

[7] S. James, R. Raheb, A. Hudak "Impact of Packet Loss to the Motion of Autonomous UAV Swarms" 39th Digital Avionics Systems Conference (DASC) October 13-15, 2020

[8] M. Johnson, E. Mueller, C. Santiago "Characteristics of a Well Clear Definition and Alerting Criteria for Encounters between UAS and Manned Aircraft in Class E Airspace" January 2015 https://aviationsystems.arc.nasa.gov/publications/2015/ATM2015_Johnson.pdf

[9] C. Goerzen, Z. Kong, and B. Mettler. "A survey of motion planning algorithms from the perspective of autonomous uav guidance". Journal of Intelligent and Robotic Systems, 57(1):65, 2009.

[10] A. Ashraf et al. "Online Path Generation and Navigation for Swarms of UAVs" December 2019, https://arxiv.org/pdf/1912.09288.pdf

[11] S. Arul et al. "LSwarm: Efficient Collision Avoidance for Large Swarms with Coverage Constraints in Complex Urban Scenes" May 2019 https://arxiv.org/pdf/1902.08379.pdf

[12] V.T. Hoang et al. "Angle-Encoded Swarm Optimization for UAV Formation Path Planning" https://arxiv.org/pdf/1812.07873.pdf

[13] A. Campello et al. "Flight Plan An Air Traffic Management Concept For Urban Air Mobility" 2030 https://daflwcl3bnxyt.cloudfront.net/m/f58fb8ea648aeb9/original/EmbraerX-White-Paper-Flight-Plan2030.pdf

[14] FAA ANG, "Version 1.0 of the Unmanned Aircraft Systems (UAS) Traffic Management(UTM) Concept of Operations" May 18, 2018, https://utm.arc.nasa.gov/docs/2018-UTM-ConOps-v1.0.pdf

[15] C. Ramsey "The Battle For Drone Tracking Technology" May 1, 2017 https://uavionix.com/the-battle-for-drone-tracking-technology/

[16] A. Weinert et al. "Well-Clear Recommendation for Small Unmanned AircraftSystems Based on Unmitigated Collision Risk" July 2018, https://arc.aiaa.org/doi/pdf/10.2514/1.D0091

[17] A. Weinert et al. "A Quantitatively Derived NMAC Analog for Smaller Unmanned Aircraft Systems Based on Unmitigated Collision Risk" November 2020 https://www.google.com/url?sa=t&rct=j&q=&esrc=s&source=web&cd=&cad=rja&uact=8&ved=2ahUKEwjR8sLTkZrvAhWKpFkKHVf-BNYQFjABegQIAhAD&url=https%3A%2F%2Fwww.preprints.org%2Fmanuscript%2F202011.0503%2Fv1%2Fdownload&usg=AOvVaw2sLsLz_eZFMxnnz5bTzWwB